J. Plasma Physics (2015), 345810101
doi:10.1017/S0022377814000695

Flow structure formation in an ion-unmagnetized plasma: The HYPER-II experiments

K. Terasaka[1]†, M. Y. Tanaka[1], S. Yoshimura[2], M. Aramaki[3], Y. Sakamoto[1], F. Kawazu[1], K. Furuta[1], N. Takatsuka[1], M. Masuda[1] and R. Nakano[1]

[1]Interdisciplinary Graduate School of Engineering Sciences, Kyushu University, 6-1 Kasuga-koen, Kasuga, Fukuoka, 816-8580, Japan
[2]National Institute for Fusion Science, 322-6 Oroshi-cho, Toki, Gifu, 509-5292, Japan
[3]College of Industrial Technology, Nihon University, 1-2-1 Izumi-cho, Narashino, Chiba, 275-8575, Japan

(Received 31 July 2014; accepted 10 August 2014; first published online 10 September 2014)

The HYPER-II device has been constructed in Kyushu University to investigate the flow structure formation in an ion-unmagnetized plasma, which is an intermediate state of plasma and consists of unmagnetized ions and magnetized electrons. High density plasmas are produced by electron cyclotron resonance heating, and the flow field structure in an inhomogeneous magnetic field is investigated with a directional Langmuir probe method and a laser-induced fluorescence method. The experimental setup has been completed and the diagnostic systems have been installed to start the experiments. A set of coaxial electrodes will be introduced to control the azimuthal plasma rotation, and the effect of plasma rotation to generation of rectilinear flow structure will be studied. The HYPER-II experiments will clarify the overall flow structure in the inhomogeneous magnetic field and contribute to understanding characteristic feature of the intermediate state of plasma.

1. Introduction

Plasmas in inhomogeneous magnetic fields are ubiquitously found in nature, and clarifying dynamical behavior of the plasmas in these fields is becoming an important issue to understand astrophysical phenomena and to develop plasma propulsion systems. When the magnetic field is strong enough and its inhomogeneity is weak, both the ions and electrons are frozen to the magnetic field line (magnetized state). However, in inhomogeneous magnetic fields, plasmas inevitably takes an intermediate state in which the ions are unmagnetized and the electrons are still strongly magnetized. In this circumstance, the mechanism of flow generation in plasmas is essentially different from that in magnetized plasmas.

Although the physics of intermediate plasmas play an essential role in plasma flow structure formation in astrophysical environments, it has not been fully understood yet. Furthermore, in an inhomogeneous magnetic field, it is interesting to note that generalized momentum or angular momentum of the magnetic field may affect the dynamical behavior of an intermediate plasma, and then, a variety of physics will

† Email address for correspondence: terasaka@aees.kyushu-u.ac.jp

arise due to interplay between the generalized field quantities and the dynamical quantities of the plasma.

In the previous experiments done in the HYPER-I device at the National Institute for Fusion Science (Tanaka et al. 1998), we have observed ion streamline detachment from the magnetic field line in an electron cyclotron resonance (ECR) plasma. From the absolute ion flow velocity measurement with the calibrated directional Langmuir probe (DLP), it has been found that the streamline detachment takes place in a diverging magnetic field, and also found that an azimuthal plasma rotation is generated according the detachment of streamline (Terasaka et al. 2010a,b). Occurrence of flow linearity and onset of azimuthal rotation are considered to be characteristic nature of intermediate plasma, and should be investigated in a larger volume to verify them as common property of intermediate state of plasma.

The HYPER-II device has been completed in July 2013, and the experiments have been started in April 2014. The HYPER-II device consists of a plasma production chamber and a large-volume diffusion chamber. A high density magnetized plasma is produced by electron cyclotron resonance (ECR) heating and is injected into the diffusion chamber with a weaker magnetic field. Intermediate plasmas are produced in the diffusion chamber, and the flow velocity field is measured with the directional Langmuir probe (DLP) method and the laser-induced fluorescence (LIF) method. The HYPER-II device is also designed for easy access of the diagnostic systems, and the diffusion chamber can be separated from the plasma production chamber to install biasing electrodes to control the plasma potential. Plasma rotation control experiments are now under progress.

The ion non-adabaticity parameter of HYPER-II plasma is extended by one order of magnitude from our previous work with the HYPER-I experiment, and we can study the whole flow structure in an inhomogeneous magnetic field. Furthermore, it is worth pointing out that flow energy of intermediate plasma becomes comparable to the magnetic field energy, and interaction between the plasma flow and the electromagnetic field may generate magnetohydrodynamics (MHD) effects. Therefore, studying the flow structure formation in an intermediate plasma is attractive from a viewpoint of physics interest as well as application interest. The knowledge obtained from the HYPER-II experiments will contributes to understand the astrophysical phenomena (Kulsrud 1994; Ji and Balbus 2013) and also to develop plasma propulsion systems (Arefiev and Breizman 2008; Schmit and Fisch 2009).

In this paper, we describe the HYPER-II device and the results of preliminary experiment. In Sec. 2, the device parameters and the diagnostic systems including the preliminary results are presented. Future experiment using the intermediate plasma is briefly described in the last section.

2. HYPER-II experiments

2.1. *Device parameters of HYPER-II*

The HYPER-II device is designed to realize a large-volume intermediate plasma and consists of two cylindrical vacuum chambers with different radii: one is the plasma production chamber with $D = 0.3$ m in diameter and $L_D = 0.95$ m in axial length, and the other is the diffusion chamber with $D = 0.76$ m and $L_D = 1.3$ m as shown in Fig. 1. These chambers are linearly arranged along the center axis of the device, and can be separated into two parts by a moving mechanics. Eight magnetic coils located around the plasma production chamber produce a magnetic beach configuration for the electron cyclotron wave (ECW) in the plasma. A steady-state plasma is produced

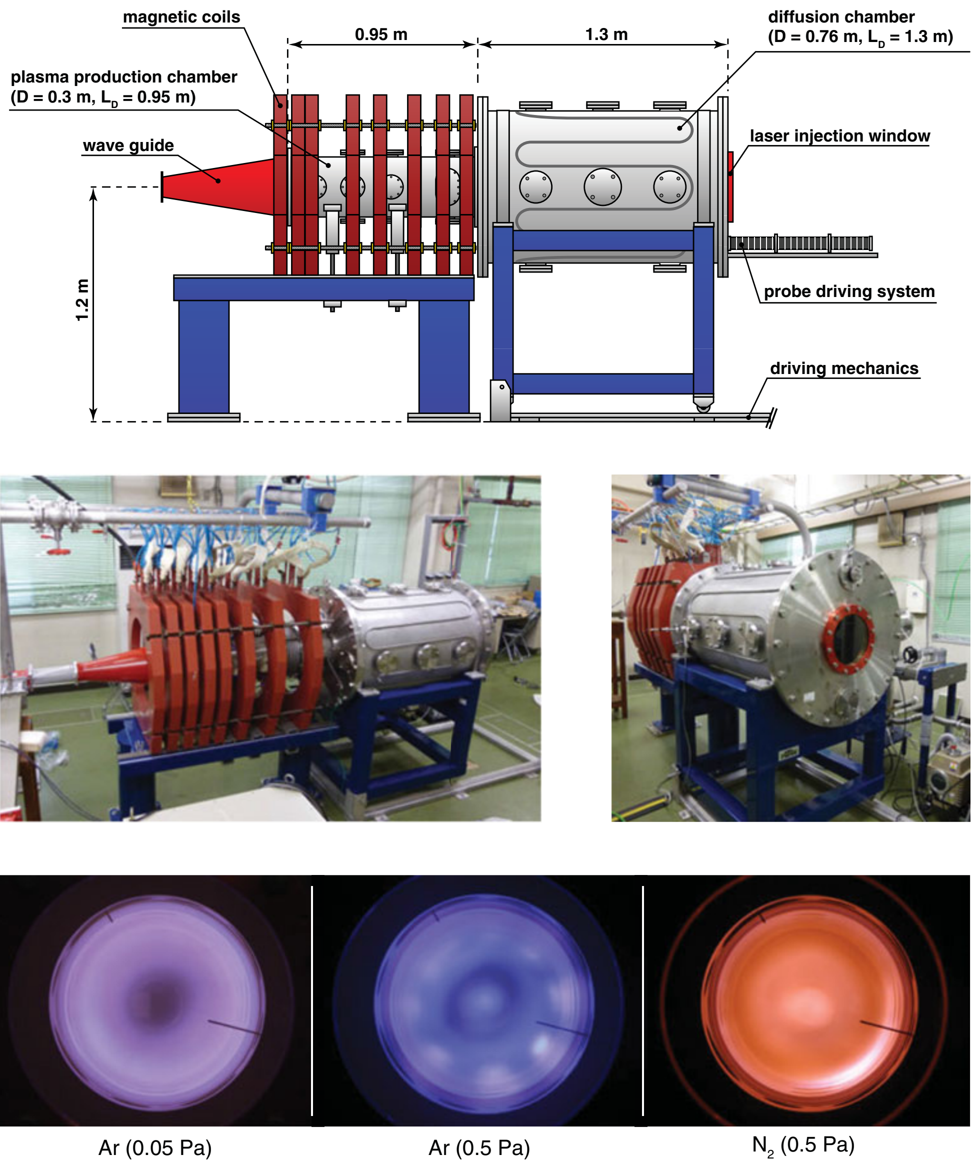

FIGURE 1. The HYPER-II system: A schematic diagram of the HYPER-II device (top); the side-view of the device (middle left) and the end-view (middle right); three typical plasma images (bottom).

by ECR heating with a microwave of frequency 2.45 GHz ($\leqslant$ 10 kW, CW), which is injected from the open end of the plasma production chamber. Since the ECW is accessible to an arbitrary dense plasma, we can easily obtain high density ECR plasmas exceeding the critical density of ordinary wave (Tanaka et al. 1991). The parameters of HYPER-II system are listed in Table 1.

Figure 2 shows the input microwave power dependences of (a) the electron density and (b) the electron temperature measured with a Langmuir probe in the diffusion chamber located at the plasma center and the axial distance of 1.3 m from the microwave launching position. Argon gas pressures without plasma are 0.01 Pa and

Plasma production chamber	$D = 0.3$ m $\times$ $L_D = 0.95$ m
Diffusion chamber	$D = 0.76$ m $\times$ $L_D = 1.3$ m
Microwave	2.45 GHz ($\leqslant$ 10 kW, CW)
Magnetic field strength	< 0.12 T
Magnetic field inhomogeneity (L_B)	$\geqslant 0.1$ m
Gas species	Ar, He, Ne, N_2 etc.
Plasma density	$\leqslant 10^{18}$ m^{-3}
Electron temperature	1-10 eV
Diagnostic systems	Langmuir probe, DLP, LIF, ICCD camera etc.

TABLE 1. Parameters of HYPER-II system.

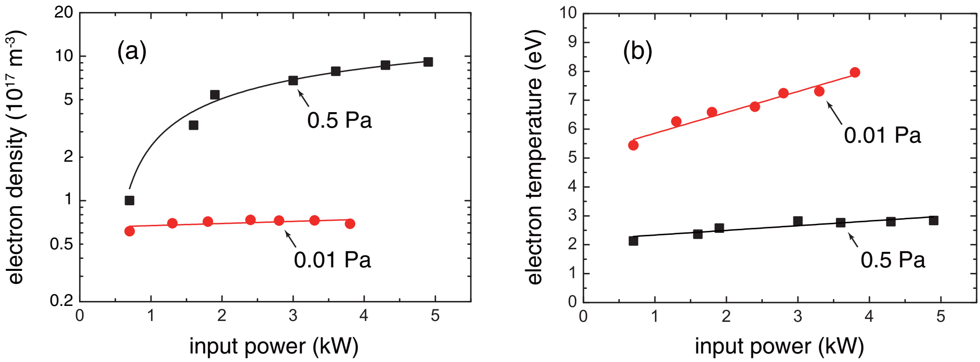

FIGURE 2. Input microwave power dependences of (a) electron density and (b) electron temperature the argon gas pressure of 0.01 Pa and 0.5 Pa in the diffusion chamber.

0.5 Pa. In the high gas pressure operation (0.5 Pa), the electron density increases with increasing the input power. The density reaches 9×10^{17} m^{-3} at 4.9 kW and is one order of magnitude higher than the critical density of ordinary wave (7.5×10^{16} m^{-3}). When the density is increasing with the input power, the electron temperature is almost constant with 2.5 eV. While in the low pressure case, the electron density is constant with increasing the input microwave power, and the electron temperature increases with increasing the input power.

The input power dependence of electron density and temperature found in Fig. 2 is qualitatively explained by the difference of dominant dissipation process of electrons. When the absorbed power of microwave in ECR heating is effectively dissipated to the ionization process between electrons and neutral particles, it is considered that the electron density increases with the input microwave power (ionization-dominant regime). On the other hand, when the energy of microwave effectively dissipated into electron-electron collisions, the electron temperature increases with the input power (heating-dominant regime). These discharge regimes appear depending on whether or not the mean free path of ionization collision is shorter than the electron-electron collision mean free path.

Figure 3(a) shows the axial profile of magnetic field strength, B. The ECR magnetic field for 2.45 GHz microwave ($B_{ECR} = 0.0875$ T) is indicated by a horizontal line. In the diffusion chamber, the maximum magnetic field is about 0.04 T, and the field decreases until the order of 10^{-3} T, which is about one tenth the minimum magnetic field realized in the HYPER-I device. The non-adiabaticity parameter, $|f_{ci}L_B/U|$, becomes an order 10^{-2} indicating the realization of a large volume of

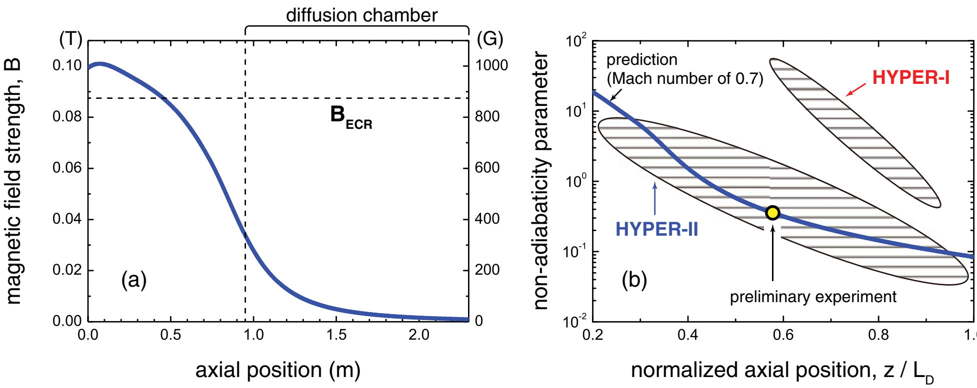

FIGURE 3. (a): Axial profile of the magnetic field strength in the HYPER-II device. A horizontal dashed line indicates the ECR magnetic field strength, $B_{\mathrm{ECR}} = 0.0875$ T. (b): Non-adiabaticity parameter as a function of axial position normalized by the device length, L_{D} (2.0 m for the HYPER-I and 2.25 m for the HYPER-II). The experimental regions are shown by hatched regions. A solid line is the non-adiabaticity parameter at the axis of HYPER-II device calculated by assuming the ion Mach number of 0.7 (typ. value).

intermediate plasma, where f_{ci} is the ion cyclotron frequency, $L_{\mathrm{B}} = [(1/B)(\mathrm{d}B/\mathrm{d}z)]^{-1}$ the characteristic scale length of the magnetic field, and U the ion flow velocity parallel to the magnetic field line. Figure 3(b) shows the values of ion non-adiabaticity parameter in the HYPER-I and the HYPER-II devices as a function of axial distance normalized by each axial device length. In the previous experiments carried out in the HYPER-I device, the ion streamline detachment from the magnetic field line has been observed in the region $0.7 \leqslant z/L_{\mathrm{D}} \leqslant 0.9$. The estimated non-adiabaticity parameter is calculated by assuming ion Mach number of 0.7 and is also shown by a solid line in the figure. The expected non-adiabaticity parameter of ions at the center of HYPER-II device is one or two order of magnitude smaller than that of HYPER-I device.

2.2. *Flow velocity measurement with a directional Langmuir probe (DLP)*

Flow velocity measurement is carried out by two diagnostic methods, i.e., DLP method and LIF method. The DLP is based on the symmetric property of directional ion current with respect to the ion flow direction and determines the ion flow velocity normalized by the ion sound speed, i.e., ion Mach number (Nagaoka et al. 2001). The DLP method provides the simplest way to measure the flow velocity and possesses a high spatial resolution. Using this method, we can easily obtain the spatial profile of flow field by moving the probe. It is worth pointing out that since the DLP gives relative Mach number, a different diagnostic procedure to calibrate the DLP is needed to measure the absolute ion flow velocity. Furthermore, electrostatic probe measurement in a plasma flowing near the ion sound velocity is not reliable. Thus, we adopt LIF spectroscopy as the calibration for the exact flow velocity determination.

In an argon plasma, the ion flow velocity has been measured on the center axis of the diffusion chamber, where the magnetic field strength is $B = 1.1 \times 10^{-2}$ T. The calibration factor is assumed to be 1 for simplicity. The result indicates that the axial flow of Mach number 0.7 (flow velocity of 2.9 km/s) is generated. This ion flow velocity gives an ion non-adiabaticity parameter of 0.3, and the ion streamline detachment is expected to take place in the large volume of diffusion chamber.

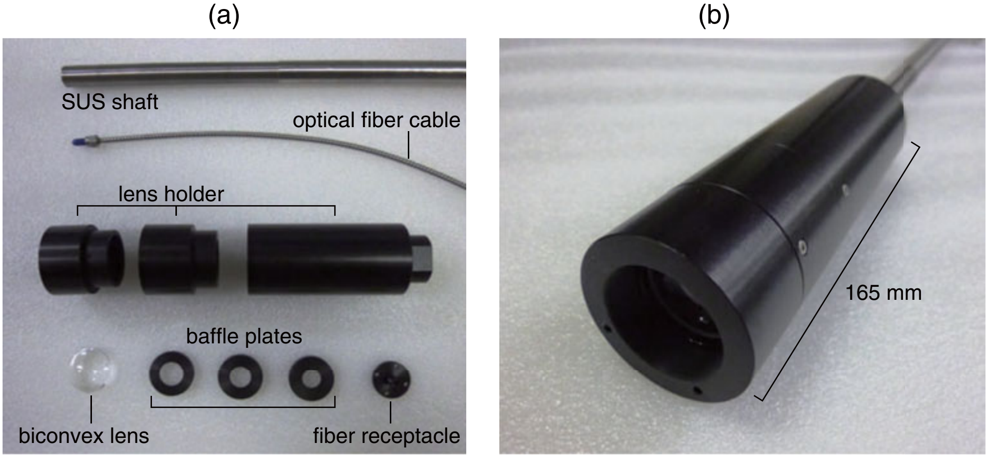

FIGURE 4. Pictures of movable LIF detector; (a): each parts and (b): overview of the detector.

2.3. *Laser induced fluorescence (LIF) spectroscopy*

The LIF method measures the population of target particles satisfying resonance absorption condition (Stern and Johnson III 1975; Engeln et al. 2001). When a tunable laser with narrow spectral band width is used as a probe beam, the velocity distribution function of target particles can be measured by tuning the laser frequency. According to the formula of Doppler shift, the absolute flow velocity is determined from the obtained LIF spectrum (velocity distribution function). The temperature is also obtained from the width of the LIF spectrum. In this method, there is no limitation of applicability like electrostatic probe method, and we can accurately determine the absolute flow velocity even in a supersonic flow. Furthermore, the LIF method can also measure the velocity distribution function of neutral particles in the plasma. The LIF method is a powerful tool to visualize the flow velocity field of the plasma and the coexistent neutral particles as well.

The accuracy of LIF method for flow velocity measurement is remarkably high. By combining the saturated absorption spectroscopy and the LIF method, we have developed a very high accuracy LIF system, and demonstrated that the velocity of neutrals of the order of 10 m/s can be measured (Aramaki et al. 2009). In the conventional LIF system, the collection optics is located outside the chamber to easily manipulate the optical signals. In HYPER-II experiments, however, it is difficult to attain a sufficient signal-to-noise ratio using conventional LIF optics, because the distance between the collection optics and the laser beam is long in the diffusion chamber. To collect an intense signal, we have developed a movable collection optics, which is located inside the plasma and makes a large solid angle against the laser irradiated plasma. Figure 4 shows the parts of the lens holder of collection optics [Fig. 4(a)] and the assembled lens head [Fig. 4(b)]. The size of lens holder is 45 mm in diameter and 165 mm in axial length, and it is supported by a stainless pipe of 15 mm in diameter, which enables us to move the lens holder using a gauge port. A biconvex lens (30 mm in diameter) is set at 10 mm behind the tip of the holder, and the collected LIF signal is focused on the end face of an optical fiber. A set of baffle plates is also used to eliminate stray lights.

Figure 5(a) shows the schematic diagram of the movable LIF system. A tunable diode laser is used as a probe laser. The laser beam is divided to a main beam (96%

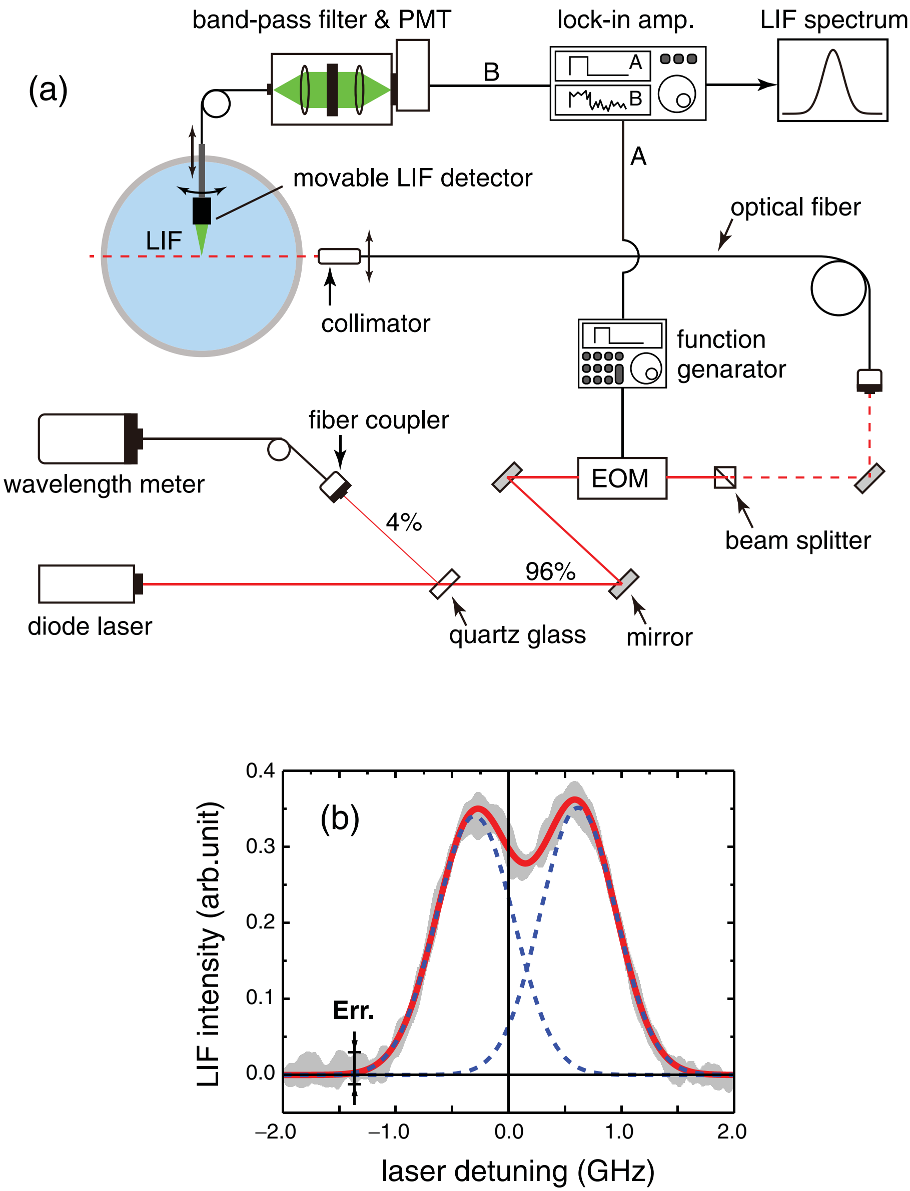

FIGURE 5. (a): Schematic diagram of the LIF measurement system. (b): Typical LIF spectrum of metastable argon atom in the diffusion chamber of HYPER-II device.

of the laser output) and a reference beam (4%). The main beam is modulated by an electro-optic modulator (EOM) and then introduced into the plasma. The position of laser beam is changed by moving the position of collimator, and the LIF signal is collected by changing the angle of the movable LIF detector. The reference beam is used to measure the laser wavelength. The LIF signal is lock-in detected to suppress the noises from the plasma. Figure 5(b) shows a typical LIF spectrum for Ar-I atoms, where the laser beam of 772.63 nm excites the metastable argon neutrals, and the de-excitation emission of 826.68 nm is detected as the LIF signal. The main laser beam is axially introduced from the laser injection window. In the present experiment, the

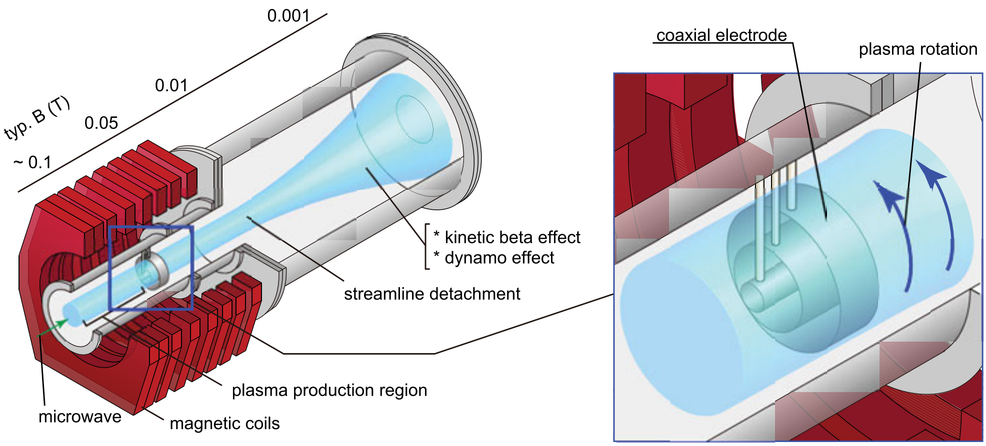

FIGURE 6. Rotation control experiment in the HYPER-II device.

split LIF spectrum, which is caused by the Zeeman effect, is obtained. By fitting the experimental data to a double-peak Gaussian function (solid line), we can determine the flow velocity by the Doppler shift of spectrum, the temperature by the spectral width, and the magnetic field strength by the peak separation. It is found that the axial flow velocity and temperature of argon atom is about 100 m/s and almost the same with the room temperature, respectively.

3. Discussions and conclusion

We have completed the HYPER-II device at Kyushu University in 2013, and started experiments on flow structure formation in an intermediate plasma. A high-density plasma is generated in the plasma production chamber, and the magnetized plasma flows along the magnetic field line into the diffusion chamber. The HYPER-II device is designed to extend the experimental region on the ion non-adiabaticity parameter, and the parameter in the HYPER-II device is one order of magnitude smaller than that in the previous experiment. The flow velocity is measured with the DLP and the newly developed LIF system, and the preliminary results indicate that an intermediate plasma is successfully generated. The flow structure formation of intermediate plasma will be clarified by the HYPER-II experiments.

In order to study the flow structure formation in an intermediate plasma, we are planning an experiment with a set of coaxial cylindrical electrodes. The schematic view of experimental apparatus is shown in Fig. 6. The electrode consists of three cylindrical shape (diameters are 30 mm, 90 mm, and 150 mm) and independently extract the current from the plasma. The electrode is set near the ECR point to efficiently control the rotation profile. A radial electric field is induced by biasing the electrodes, and the azimuthal plasma rotation due to $\boldsymbol{E} \times \boldsymbol{B}$ drift is induced, where $\boldsymbol{E}$ is the electric field in the plasma. Effect of plasma rotation in the magnetized region on the flow structure in intermediate plasma, e.g., the acceleration of rotating plasma, will be studied by measuring the flow structure in the diffusion chamber with the DLP method and the new LIF method. When a radial electric field of the order of a few V/cm is produced, the kinetic energy of rotation is almost the same as that of axial flow, and the effect of plasma rotation on the axial flow structure formation will be remarkable.

It is worth pointing out that the plasma beta values become an order of 0.1 in the diffusion chamber of HYPER-II, and such the high beta plasma has not been generally realized. The HYPER-II experiments make possibility us to investigate the fundamental physics of various astrophysical phenomena such as stretching of magnetic field line and magnetic-dynamo effect in a laboratory plasma. The knowledge of intermediate plasma will contribute as a fundamental physics in developing plasma propulsion systems and also as a laboratory experiment concerning astrophysical phenomena.

Acknowledgement

This work was supported by JSPS KAKENHI Grant Numbers 23244112 and 25800306.

REFERENCES

Aramaki, M., Ogiwara, K., Eto, S., Yoshimura, S. and Tanaka, M. Y. 2009 High resolution laser induced fluorescence doppler velocimetry utilizing saturated absorption spectroscopy. *Rev. Sci. Instrum.* **80**, 053505 1–4.

Arefiev, A. V. and Breizman, B. N. 2008 Ambipolar acceleration of ions in a magnetic nozzle. *Phys. Plasmas* **15**, 042109 1–8.

Engeln, R., Mazouffre, S., Vankan, P., Schram, D. C. and Sadeghi, N. 2001 Flow dynamics and invasion by background gas of a supersonically expanding thermal plasma. *Plasma Sources Sci. Technol.* **10**, 595–605.

Ji, H. and Balbus, S. 2013 Angular momentum transport in astrophysics and in the lab. *Phys. Today* **66**, 27–33.

Kulsrud, R. M. 1994 Important plasma problems in astrophysics. *Phys. Plasmas* **2**, 1735–1745.

Nagaoka, K., Okamoto, A., Yoshimura, S. and Tanaka, M. Y. 2001 Plasma flow measurement using directional langmuir probe under weakly ion-magnetized conditions. *J. Phys. Sco. Jpn.* **70**, 131–137.

Schmit, P. F. and Fisch, N. J. 2009 Magnetic detachment and plume control in escaping magnetized plasma. *J. Plasma Phys.* **75**, 359–371.

Stern, R. A. and Johnson III, J. A. 1975 Plasma ion diagnostics using resonant fluorescence. *Plasma Sources Sci. Technol.* **34**, 1548–1551.

Tanaka, M., Nishimoto, R., Higashi, S., Harada, N., Ohi, T., Komori, A. and Kawai, Y. 1991 Overdense plasma production using electron cyclotron waves. *J. Phys. Sco. Jpn.* **60**, 1600–1607.

Tanaka, M. Y., Bacal, M., Sasao, M. and Kuroda, T. 1998 High-density plasma production for neutralizing negative ion beam. *Rev. Sci. Instrum.* **69**, 980–982.

Terasaka, K., Yoshimura, S., Ogiwara, K., Aramaki, M. and Tanaka, M. Y. 2010a Experimental studies on ion acceleration and stream line detachment in a diverging magnetic field. *Phys. Plasmas* **17**, 072106 1–6.

Terasaka, K., Yoshimura, S., Ogiwara, K., Aramaki, M. and Tanaka, M. Y. 2010b Self-calibrated measurement of ion flow using a fine multihole directional langmuir probe. *Japan. J. Appl. Phys.* **49**, 036101 1–6.